CME ARTICLE
REVIEW ARTICLE

Myocardial blood flow: Putting it into clinical perspective

Thomas Hellmut Schindler, MD[a]

[a] Division of Nuclear Medicine, Cardiovascular Nuclear Medicine, Department of Radiology and Radiological Science SOM, Johns Hopkins University School of Medicine, Baltimore, MD

Received Nov 30, 2015; accepted Dec 1, 2015
doi:10.1007/s12350-015-0372-4

In recent years, positron emission tomography/computed tomography (PET/CT)-determined myocardial perfusion in conjunction with myocardial blood flow (MBF) quantification in $mL \cdot g^{-1} \cdot min^{-1}$ has emerged from mere research application to initial clinical use in the detection and characterization of the coronary artery disease (CAD) process. The concurrent evaluation of MBF during vasomotor stress and at rest with the resulting myocardial flow reserve (MFR = MBF during stress/MBF at rest) expands the scope of conventional myocardial perfusion imaging not only to the detection of the most advanced and culprit CAD, as evidenced by the stress-related regional myocardial perfusion defect, but also to the less severe or intermediate stenosis in patients with multivessel CAD. Due to the non-specific nature of the hyperemic MBF and MFR, the interpretation of hyperemic flow increases with PET/CT necessitates an appropriate placement in the context with microvascular function, wall motion analysis, and eventually underlying coronary morphology in CAD patients. This review aims to provide a comprehensive overview of various diagnostic scenarios of PET/CT-determined myocardial perfusion and flow quantification in the detection and characterization of clinically manifest CAD.

Key Words: CAD • myocardial ischemia • myocardial blood flow • myocardial flow reserve • multivessel disease • positron emission tomography • left ventricular wall motion

Abbreviations

ACE-I	Angiotensin-converting enzyme inhibitors
ARB	Angiotensin II receptor blockers
CABG	Coronary artery bypass grafting
CAD	Coronary artery disease
CT	Computed tomography
MBF	Myocardial blood flow
MFR	Myocardial flow reserve
PET	Positron emission tomography
PTCA	Percutaneous transluminal coronary angioplasty
SPECT	Single-photon emission tomography

Reprint requests: Thomas H. Schindler, MD, Division of Nuclear Medicine, Cardiovascular Nuclear Medicine, Department of Radiology and Radiological Science SOM, Johns Hopkins University School of Medicine, JHOC 3225, 601 N. Caroline Street, Baltimore, MD 21287; *tschind3@jhmi.edu*
J Nucl Cardiol 2016;23:1056–71.
1071-3581/$34.00
Copyright © 2015 American Society of Nuclear Cardiology.

INTRODUCTION

In recent years, positron emission tomography (PET)-determined myocardial perfusion in conjunction with myocardial blood flow (MBF) quantification in $mL \cdot g^{-1} \cdot min^{-1}$ has translated from research application to initial clinical use in the detection and characterization

Table 1. Scope of PET/CT-determined hyperemic MBF and MFR

1. Identification and characterization of subclinical CAD
2. Incremental predictive value on future cardiovascular outcome
3. Assessment of microvascular disease in symptomatic patients without or with non-obstructive CAD*
4. CAD detection in advanced obesity*
5. Characterization of the extent and severity of CAD burden in multivessel disease*
6. Detection of diffuse ischemia owing to significant left main stem and/or three-vessel CAD*,†

CAD, coronary artery disease; *CT*, computed tomography; *MBF*, myocardial blood flow; *MFR*, myocardial flow reserve; *PET*, positron emission tomography
*Common clinical indications
†Effects of diffuse myocardial ischemia should be confirmed by a peak stress transient cavity dilation of the left ventricle during maximal vasomotor stress on gated PET images

of the coronary artery disease process (CAD).[1-6] Quantification of MBF at rest and during pharmacologically induced hyperemia with PET or PET/CT affords the non-invasive identification of coronary microvascular dysfunction as early functional and subclinical stage of the CAD process (Table 1), which carries important diagnostic and prognostic information.[7-12] The assessment of microvascular dysfunction also proofs helpful to identify the potential source of angina symptoms in patients with syndrome X, arterial hypertension, diabetes mellitus, or different phenotypes of hypertrophic obstructive cardiomyopathy.[13-18] In these patients, lifestyle changes and specific medical treatment such as ACE-I, ARB, statin, anti-diabetic, medication and/or ranolazine may be installed, and response to treatment can be verified with PET/CT flow quantification.[17,19-22]

In particular, the quantification of hyperemic MBF and myocardial flow reserve (MFR = MBF during stress/MBF at rest) also expands the scope of conventional myocardial perfusion imaging from the detection of the most advanced and culprit CAD, as evidenced by the stress-related regional myocardial perfusion defect, to the less severe but intermediate stenosis in patients with multivessel disease (Table 1).[1,2,23,24] Yet, in view of the relatively low specificity of the hyperemic MBF and/or MFR,[24,25] the interpretation of stress-related MBFs with PET/CT needs to be placed in the context with microvascular (dys)function, wall motion analysis, and eventually underlying coronary morphology in CAD patients.[1,3,26]

This review aims to provide a comprehensive overview of various diagnostic scenarios of PET/CT-determined myocardial perfusion and flow quantification in the detection and characterization of clinically manifest CAD.

INTERRELATION BETWEEN EPICARDIAL STENOSIS AND FLOW

With the introduction of PET-determined myocardial perfusion in conjunction with MBFs in clinical practice, an appreciation of coronary pathophysiology has regained a central role in the diagnostic and decision-making process for treatment options in CAD patients. Seminal investigations from Gould et al[27-30] followed by other investigators[31-33] have untraveled the interrelation between structural and functional determinants of CAD. As it was observed, pharmacologically stimulated hyperemic MBFs commonly decreased in the presence of a coronary narrowing exceeding 50% of luminal diameter (Figure 1).[31-34] Although there is a well-known inverse relationship between severity of CAD lesions and MFR, individual hyperemic flows may vary substantially due to different degree of adaptive vasodilator response of the coronary arteriolar vessels to balance CAD lesion-induced increase in epicardial resistance and/or the presence of collateral flow.[15,35,36] These observations also accord with a more recent comparative study between CT-determined luminal epicardial stenosis and stress-induced regional myocardial perfusion defects as determined with ^{201}Thallium SPECT.[37] Stress-related regional myocardial perfusion defects were appreciated in 33% of regions with 60% to 70% stenosis, 54% of regions with 70% to 80% stenosis, and 86% of regions with ≥80% stenosis. Thus, even in the range of epicardial lesions between 70% and 80% in about half of these lesions, no regional perfusion defects were noted. The ultimate effect of an epicardial stenosis is stringent on the extent to which the increase in epicardial resistance to hyperemic flows caused by the stenosis is indeed balanced by the capacity or ''reserve'' of the arteriolar vessels to dilate.[29,30] The coronary vasodilator capacity may be appreciated as an auto-regulatory system, e.g., the ability of the coronary circulation to maintain the flow at a constant level despite a decrease in coronary pressure for a given myocardial metabolic demand. The flow reserve, however, decreases as coronary pressure declines and becomes exhausted when coronary pressure attains a level at which auto-regulatory vasodilation is maximal

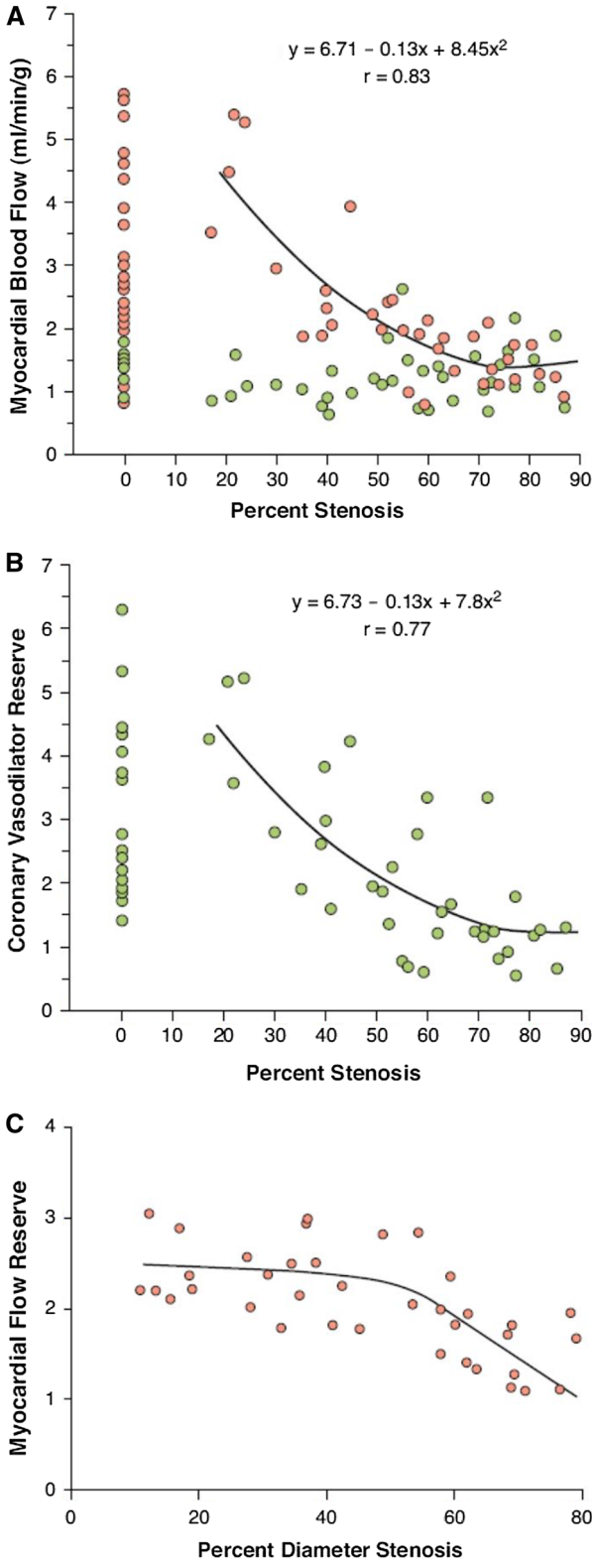

Figure 1. MBF and coronary flow reserve in relation to epicardial artery diameter stenosis (%). (**A**) No relationship between myocardial blood flow (MBF) and percentage coronary artery stenosis at rest (*green circles*) is observed. Conversely, there is an inverse relationship between hyperemic MBFs and percentage of focal epicardial narrowing during pharmacologic vasodilation (*red circles*). (**B**) As described for hyperemic MBFs, myocardial (or coronary) flow reserve (MFR = hyperemic MBF/resting MBF) displays a comparable inverse relationship with percentage coronary artery stenosis.[31] When looking at stenoses of intermediate severity (40% to 70% diameter stenosis), however, a relatively high variability in MFR values is observed. Importantly, reductions in hyperemic MBF or MFR in individuals without epicardial coronary artery stenoses may be similar to those in myocardial regions subtended to epicardial lesions ≥50% diameter stenosis. (**C**) MFR commonly declines when percent diameter stenosis exceeds ≥50% as assessed with quantitative coronary angiography (correlation coefficient $r = 0.77$, root mean square error = 0.37, $P < .00001$)[32] (reproduced with permission from reference[1]).

(Figure 2).[29,31,32,38-41] Thus, relatively maintained regional hyperemic MBF or MFR may indeed counterbalance the manifestation of stress-induced myocardial ischemia that again explains the relatively low prevalence of only about 30% of myocardial ischemia in the presence of epicardial narrowing >50%.[42] In addition, the presence of sufficient flow owing to the hypoxic stimulus of the disbalance between myocardial oxygen demand and supply may contribute to the prevention of clinically manifest ischemic heart disease.[15,35,40,41] Conceptually, as HMG-CoA reductase or angiotensin-converting enzyme inhibitors have been demonstrated to improve the coronary vasodilator capacity,[1,3,43-45] they may prevent or even resolve myocardial ischemia in CAD patients with secondary preventive medical care. This contention may conform to clinical findings of a subanalysis of the clinical outcomes utilizing revascularization and aggressive drug evaluation (COURAGE) trial.[46] Medical treatment of cardiovascular risk factors with HMG-CoA reductase or ACE inhibitors in patients with SPECT-determined regional myocardial perfusion defects over a 1-year follow-up did indeed lead to a significant reduction in ischemic burden associated with a favorable clinical outcome.[46]

NON-SPECIFICITY OF HYPEREMIC MBF

Although PET-determined hyperemic MBFs and MFR advance the identification and characterization of multivessel CAD, the relatively low specificity of abnormal hyperemic flows per se does not afford the discrimination between stress-induced diffuse ischemia owing to left main and/or multivessel CAD or diffuse microvascular dysfunction as both conditions may result in diffuse and balanced reductions in hyperemic MBFs.[24,25] Conversely, normal hyperemic MBFs during pharmacologic vasodilation, such as ≥1.8 $mL \cdot g^{-1} \cdot min^{-1}$

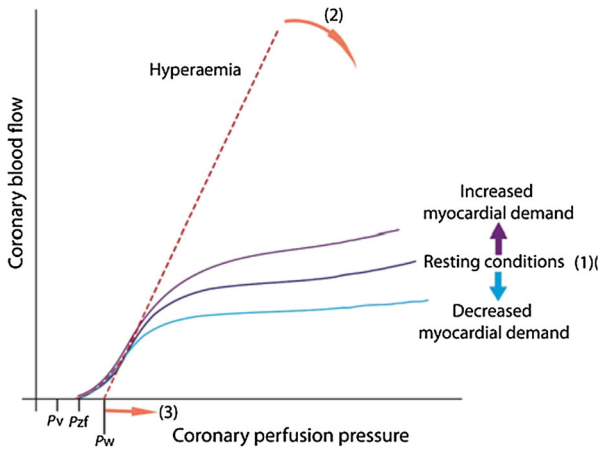

Figure 2. The coronary pressure-Flow relationship. Coronary or myocardial blood flow (MBF) at rest (*solid lines*) is regulated to match myocardial oxygen demand and to balance alterations in coronary perfusion pressure by parallel changes in microvascular resistance, resulting in an auto-regulatory plateau. This auto-regulatory control, however, becomes exhausted when the coronary arteriolar vessels are dilated to a maximum. Under such condition, the MBF is dependent on the coronary perfusion pressure only (*dotted line*). The coronary pressure-flow relationship is concave at low perfusion pressures. The zero-flow intercept on the pressure axis (Pzf) just overcomes venous pressure (Pv). Straight extrapolation of the hyperemic pressure-flow relationship manifests in an incremental-linear relationship that intercepts the pressure axis at the coronary wedge pressure (Pw), implying collateral flow, heart rate, and ventricular wall tension, which are commonly highly variable in the human coronary circulation (3). For example, microvascular dysfunction or abnormal left ventricular function decreases the slope of the pressure-flow relationship (curved arrow (2)). Conversely, increases in left ventricular end-diastolic pressure or left ventricular hypertrophy lead to a parallel shift to the right (straight arrow (3)) (reproduced with permission from reference[39]).

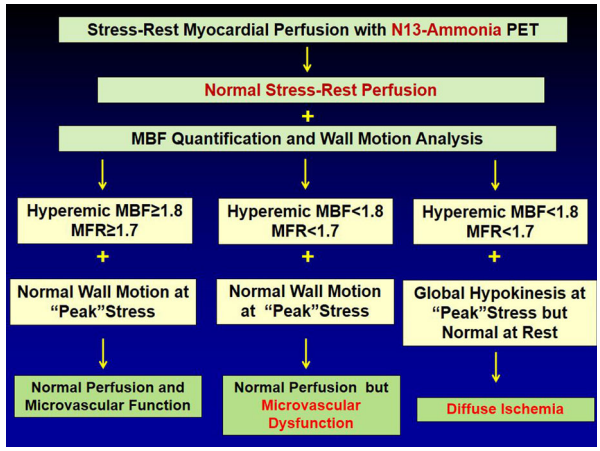

Figure 3. Algorithm for the integration of ^{13}N-ammonia PET/CT perfusion images, MBF, and wall motion analysis for differentiation between microvascular dysfunction and diffuse ischemia. Combining hyperemic MBFs and wall motion analysis at ''peak'' stress affords the differentiation between predominant microvascular dysfunction and diffuse myocardial ischemia owing to significant left main and/or three-vessel CAD. For example, balanced reductions in hyperemic MBFs and normal wall motion of the left ventricle at peak stress argue for the presence of predominantly microvascular disease but not diffuse ischemia. Conversely, diffuse reductions in hyperemic MBFs associated with transient ischemic cavity dilation (TID) of the left ventricle during vasomotor stress on gated PET images is widely specific for the presence of diffuse ischemia.[1,51,94].

for the positron flow tracer ^{13}N-ammonia or a MFR >2.0,[47] widely signify a normal 2-component system with a non-obstructive epicardial conduit artery and normal functioning coronary arteriolar vessels. In the absence of obstructive CAD, hyperemic MBFs may be abnormally reduced due to microvascular dysfunction related to adverse effects of cardiovascular risk factors, left ventricular hypertrophy, hypertrophic obstructive and non-obstructive cardiomyopathy, or hyperreactivity of the vascular smooth muscle cells in the so-called syndrome X patients.[13-16,18,19,48] While an abnormal hyperemic MBF and MFR cannot separate which of the two components accounts for the observed impairment of hyperemic flow increases,[49,50] normal hyperemic flows have a high negative predictive value of 97% in ruling out high-risk CAD as evidenced by invasive coronary angiography.[25] In contrast to PET-determined hyperemic MBFs, stress-induced regional perfusion defects afford the advantage that they specifically signify flow-limiting effects of advanced epicardial coronary artery lesions.[1,42] Of further importance is that gated PET imaging is performed at ''peak'' stress. This affords a reliable identification of transient ischemic left ventricular cavity dilation to signify diffuse ischemia[51] that otherwise may be missed with conventional ^{99m}Technetium SPECT imaging as gated image acquisition is commonly done 40-45 minute after radiotracer injection. Combining all information from the, e.g., ^{13}N-ammonia PET/CT, such as myocardial perfusion (relative radiotracer uptake), MBF, and left ventricular wall motion at peak stress and rest in patients with suspicion of CAD, however, is critical to diagnose and differentiate between cardiovascular risk factor-induced microvascular dysfunction, hemodynamic significant CAD, and diffuse myocardial ischemia owing to significant left main and/or three-vessel disease (Figure 3).

Another possibility to circumvent the non-specificity of hyperemic MBFs is the evaluation of a longitudinal decrease in hyperemic MBFs from the base to the apex of the heart that is supposed to provide information of down-stream, flow-limiting effects of epicardial stenosis, and/or impaired flow-mediated vasodilation.[24,52-57] This novel flow parameter is likely to yield more specific information on epicardial

resistance than the conventional MFR.[24,54,57-59] If this evolving concept of a decrease in longitudinal hyperemic MBF to reflect epicardial stenosis or resistance to flow is confirmed in further validation studies, then the longitudinal MBF gradient could indeed evolve to a non-invasive fractional flow reserve for evaluation of the functional severity of epicardial narrowings.[24,49]

CAD EVALUATION IN MULTIVESSEL DISEASE

As mentioned before, evaluating the relative perfusion or homogeneity of radiotracer uptake in the left ventricle during vasomotor stress aims to identify regional perfusion defects underlying flow-limiting CAD lesions. Although stress-induced regional myocardial perfusion defects afford the identification of an advanced CAD lesion or the ''culprit'' and, thus, the most advanced CAD stenosis lesion in multivessel disease, the remaining lesions of less severity or intermediate range may be missed.[60] Due to the non-specific nature of hyperemic MBFs and MFR, however, adding coronary morphology information is indispensable to relate decreases of regional hyperemic MBFs and/or MFR to each epicardial stenosis in multivessel disease (Figure 4). It is important to keep in mind that with increasing severity of a focal epicardial stenosis, the vascular resistances shift from the microcirculation to the site of epicardial stenosis as the adaptive vasodilation becomes exhausted, which may be reinforced by microvascular dysfunction. For a given epicardial stenosis, the optimal cut-off values of PET-determined hyperemic MBFs and MFR to signify abnormal hyperemic flow and, thus, the hemodynamic significance of a stenosis, however, are still a matter of ongoing debate.[1,26,61] Owing to differences in methodology and positron flow tracers applied, some variability in PET-determined MBFs exists, which has been described in detail elsewhere.[1,26,62,63] When applying ^{13}N-ammonia, the optimal threshold for hyperemic MBFs has been reported to be 1.85 mL·g^{-1}·min^{-1} in a total of 27 patients with known or suspected CAD and 21 normal individuals (Table 2).[47] In view of previous invasive investigation with intracoronary Doppler measurements of coronary flow velocities,[60,64,65] the threshold of the MFR is commonly defined as 2.0 for ^{13}N-ammonia and ^{82}Rubidium.[26,47,66,67] As regards ^{82}Rubidium as positron-emitting flow tracer, no threshold to define abnormal and normal hyperemic MBFs so far has been reported. As a consequence, the MFR threshold of 2.0 is currently used for ^{82}Rubidium to define abnormal and normal vasodilator capacity of the coronary circulation.[9,67] Another positron-emitting flow tracer is ^{15}O-water but not US Food and Drug Administration (FDA) approved for which thresholds have been well defined with 2.3 mL·g^{-1}·min^{-1} for hyperemic MBF and 2.50 for the MFR, respectively.[5,6] Regarding the potential of hyperemic flow increases in the identification of flow-limiting effects of CAD lesions, a prospective and multicenter trial in 191 patients with stable angina and multivessel CAD was performed to investigate the roles of intracoronary derived coronary flow velocity reserve (CVR) and myocardial perfusion scintigraphy with SPECT for management of an intermediate coronary lesion (40% to 70% diameter stenosis).[60] Apart from intermediate stenoses, all CAD patients had at least one severe epicardial stenosis (>70% diameter narrowing) that was accepted for PTCA. Subsequently, PTCA of the remaining intermediate lesion was deferred if SPECT was negative or CVR $\geq$2.0. Patients were followed for 1 year to document major cardiac events (death, infarction, and revascularization) and, if occurred, related to the intermediate lesion. Overall, PTCA of intermediate lesions was deferred in 182 patients with a CVR $\geq$2.0. During the one-year follow-up, nineteen major cardiovascular events occurred (three myocardial infarctions and sixteen revascularizations). CVR appeared to be more accurate and an independent predictor of cardiac events than SPECT perfusion imaging. Of particular interest, deferral of PTCA of intermediate epicardial lesions in multivessel CAD, based on a CVR $\geq$2.0, was safe with a lower event rate of 6% as compared to a relatively high event rate of 24% (relative risk 3.9%), given a reduced CVR <2.0. These observations suggest indeed that invasively measured CVR affords the evaluation of the functional severity of intermediate coronary lesion in each coronary vessel enhancing risk stratification and avoiding additional testing with myocardial perfusion scintigraphy and repeat cardiac catheterization. In support of this investigation,[60] other diagnostic investigations with Doppler flow velocity measurements also reported a safe deferral of PTCA with low event rate (5% to 10%) when CVR was normal or $\geq$2.0.[64,65] These invasive coronary flow investigations[60,64,65] provide an important framework for the current application of PET/CT perfusion and MBF measurements for the evaluation of the functional or hemodynamic severity each single epicardial lesion in CAD.[4] Cardiac PET/CT flow quantification to assess the functional significance of each epicardial lesions, therefore, may indeed emerge as non-invasive and pivotal tool in the clinical decision making to individualize coronary revascularization options with PCTA, CABG, or hybrid interventions in patients with multivessel disease.

THRESHOLDS, MBF, AND CORONARY MORPHOLOGY

As reductions in hyperemic MBFs may be similar in patients with obstructive and non-obstructive CAD, they may origin not only from flow-hampering effects of epicardial stenosis but also from cardiovascular risk

factor-induced microvascular function or both.[24,25,31,32,34] Thus, in patients with multivessel CAD, the relatively low specificity of reduced MFR necessitates information on coronary morphology for an appropriate interpretation of myocardial perfusion and regional MFR values (Figures 4, 5).[1,24,25,43] In this respect, a recent consensus paper led by Gould et al[4] has outlined that for an epicardial stenosis ≥70%, reductions in MFR <1.7 can be considered to account for significant, down-stream and flow-limiting effects of CAD lesions. Combining thresholds of the severity of coronary stenosis and MFR circumvents the non-specificity of MFR but requires further information on coronary morphology and stenosis severity. The relationship between transstenotic pressure gradient and the percent diameter stenosis is ''non-linear'', with a progressively more fast increase in pressure gradient as the degree of stenosis surpasses 70% (Figure 1).[4] When a given stenosis reaches 85% to 90%, the auto-regulatory reserve is commonly exhausted, while flow is reduced slightly under resting condition for a 90% diameter stenosis. Thus, the threshold of 70% stenosis as morphological criteria relates well to flow pathophysiology.[49,50,64,65,68] Similar to invasive observations of invasively conducted studies,[29,30,60] the combined application of abnormal thresholds with an epicardial stenosis ≥70% and MFR <1.7 enables the non-invasive characterization of the hemodynamic significance of each epicardial lesion in multivessel CAD. While a stress-induced regional myocardial perfusion defect identifies the presence of advanced CAD and the ''culprit lesion,'' a reduction of the MFR of less than 1.7 subtended to a stenosis of intermediate severity signifies flow-limiting effects even in the absence of a regional myocardial perfusion defect (Figures 4, 5). Support for the use of abnormal MFR to signify hemodynamic effects of CAD stenosis comes from several invasive validation studies measuring the post-stenotic coronary flow velocity reserve in CAD patients with stress-induced myocardial perfusion defects in the corresponding region on scintigraphic myocardial perfusion images (Table 3).[69-71]

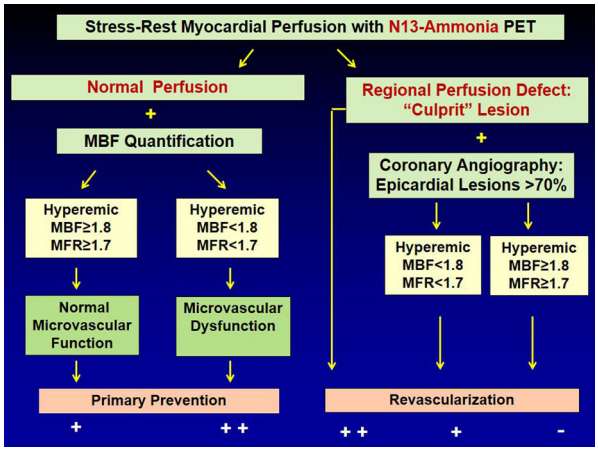

Figure 4. Algorithm for the integration of ^{13}N-ammonia PET/CT perfusion images and MBFs in multivessel CAD. In individuals with normal stress-rest myocardial perfusion images, the quantification of hyperemic MBF and MFR may unravel microvascular dysfunction as functional precursor of CAD that may reinforce lifestyle changes and/or preventive medical care. Conversely, while a stress-induced regional perfusion defect signifies the ''culprit'' or most advanced CAD lesion, added hyperemic MBF and MFR may signify flow-limiting effects of lesions >70% diameter stenosis in patients with multivessel CAD[1,4].

For example, Miller et al[69] investigated thirty-three patients with CAD were undergoing quantitative coronary angiography (QCA) with a mean percent diameter stenosis of 56% ± 14%, Doppler-derived measurements of post-stenotic hyperemic intracoronary flow reserve, and subsequently ^{99m}Tc-sestamibi myocardial perfusion imaging with SPECT during adenosine-stimulated hyperemic flows and at rest. There was a strong correlation between hyperemic distal flow velocity ratio measurements and ^{99m}Tc-sestamibi perfusion imaging results in 24 of 27 patients (89%; kappa = 0.78). In particular, all 14 patients with abnormal distal hyperemic flow velocity values (≤2.0) had corresponding reversible ^{99m}Tc-sestamibi tomographic defects. In another study, Joye et al[70] compared invasively determined coronary flow reserve to exercise-induced myocardial ischemia on ^{201}Thallium SPECT images in thirty individuals with intermediate

Table 2. Thresholds of different PET-radiotracers to define normal vs abnormal hyperemic MBF and MFR

	^{13}N-Ammonia	^{82}Rubidium	^{15}O-Water
Hyperemic MBF	1.8 mL·g^{-1}·min^{-1}	/	2.3 mL·g^{-1}·min^{-1}
MFR	2.0*	2.0*	2.5

MBF, myocardial blood flow; *MFR*, myocardial flow reserve; *N/A*, not applicable
*Commonly accepted threshold as defined by invasive investigations[60,64,65]

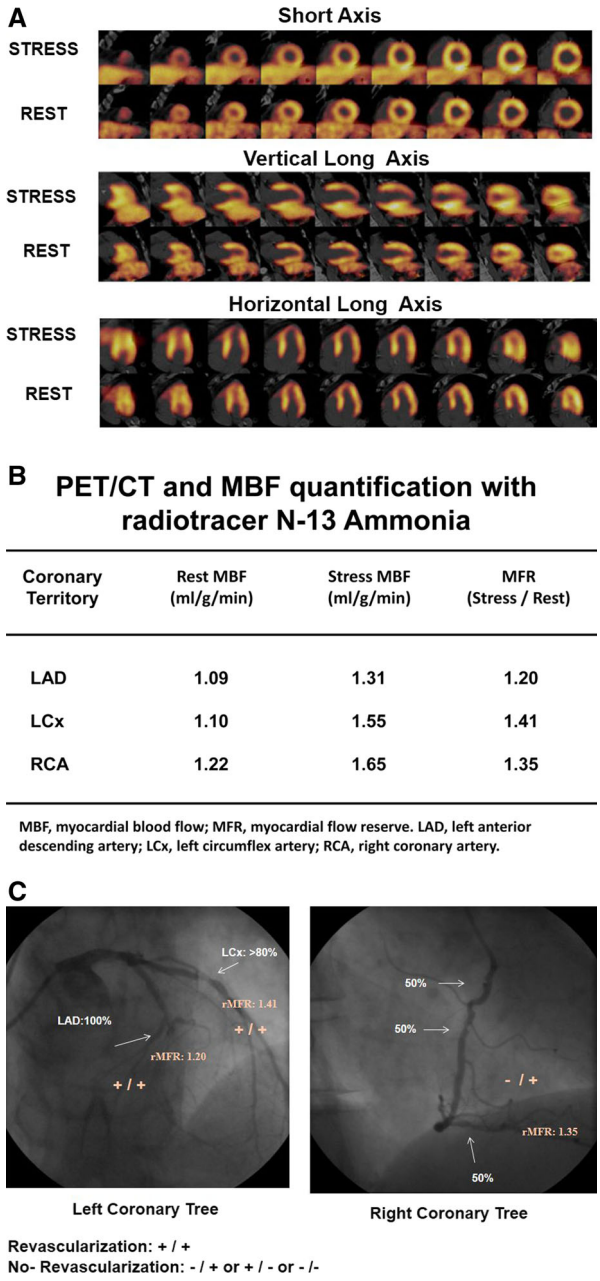

Figure 5. ^{13}N-ammonia PET/CT-determined perfusion and MBF in multivessel CAD. A 61-year-old patient who had long-standing arterial hypertension and type 2 diabetes mellitus presented with progressive shortness of breath and atypical chest pain. (**A**) On stress ^{13}N-ammonia perfusion images, there is a moderately reduced radiotracer uptake of the mid-to-distal anterior, anteroseptal, and apical regions of the left ventricle, that becomes reversible on the rest images to signify ischemia in the LAD distribution. Conversely, ^{13}N-ammonia uptake is widely preserved in the lateral and inferior regions. (**B**) Quantification of MBFs demonstrates globally reduced MFR with a regional MFR of 1.20 in the LAD, 1.41 in the LCx, and 1.35 in the RCA distribution, respectively. (**C**) Invasive coronary angiography unmask significant three-vessel disease with proximal occlusion of the LAD, 80% stenosis in the proximal segments of the LCX (left panel), and sequential 50% to 60% lesions in the RCA (right panel). When defining flow-limiting CAD with epicardial stenosis >70% and MFR <1.7 (*criteria:* +/+), apart from the proximal LAD occlusion, the LCx lesion of less and intermediate severity (≈80%) would also be regarded as hemodynamic significant despite normal radiotracer uptake. As regards the RCA, only one criterion applies. While regional MFR is markedly reduced with 1.35, the serial lesions of 50% do not reach the threshold of >70% diameter stenosis (*criteria:* ∓). Thus, the pronounced reduction in MFR in the RCA distribution may predominantly reflect microvascular dysfunction and not hemodynamically obstructive CAD (adapted and reproduced with permission from reference[1]).

coronary stenosis (40% to 70% stenosis). An abnormal coronary flow reserve ≤2.0 resulted in a sensitivity, specificity, and overall predictive accuracy of 94%, 95%, and 94%, respectively, for exercise-induced regional ischemia on ^{201}Thallium SPECT images. In a similar study conducted by Deychak et al,[71] an excellent concordance between distal coronary flow reserve and exercise-rest ^{201}Thallium SPECT perfusion imaging was reported. In this respect, a coronary flow reserve of <1.8 predicted a reversible myocardial perfusion defect on ^{201}Thallium SPECT with a concordance of 96%, outlining that a post-stenotic CVR of <1.8 is strongly suggestive of significant down-stream, flow-limiting effects of epicardial lesions ranging between 55% and 85% diameter stenosis. These single-center investigations were then followed by a

Table 3. Myocardial perfusion scintigraphy and invasively determined coronary flow velocity

Author	(*n*)	Ischemic test	CVR	Sensitivity	Specificity	PPV	NPV	Accuracy
Miller (Ref.[69])	33	Adeno/dipy MIBI	<2.0	82	100	100	77	89
Joye (Ref.[70])	30	Exercise ^{201}Thallium	<2.0	94	95	94	95	94
Dechak (Ref.[71])	17	Exercise ^{201}Thallium	<1.8	94	94	100	91	96
Heller (Ref.[72])	100	Exercise ^{201}Thallium	<1.8	89	92	96	89	92

Adeno, adenosine; *dipy*, dipyridamole; *MIBI*, sestamibi scan; (*n*), number of patients; *PPV*, positive predictive value; *NPV*, negative predictive value

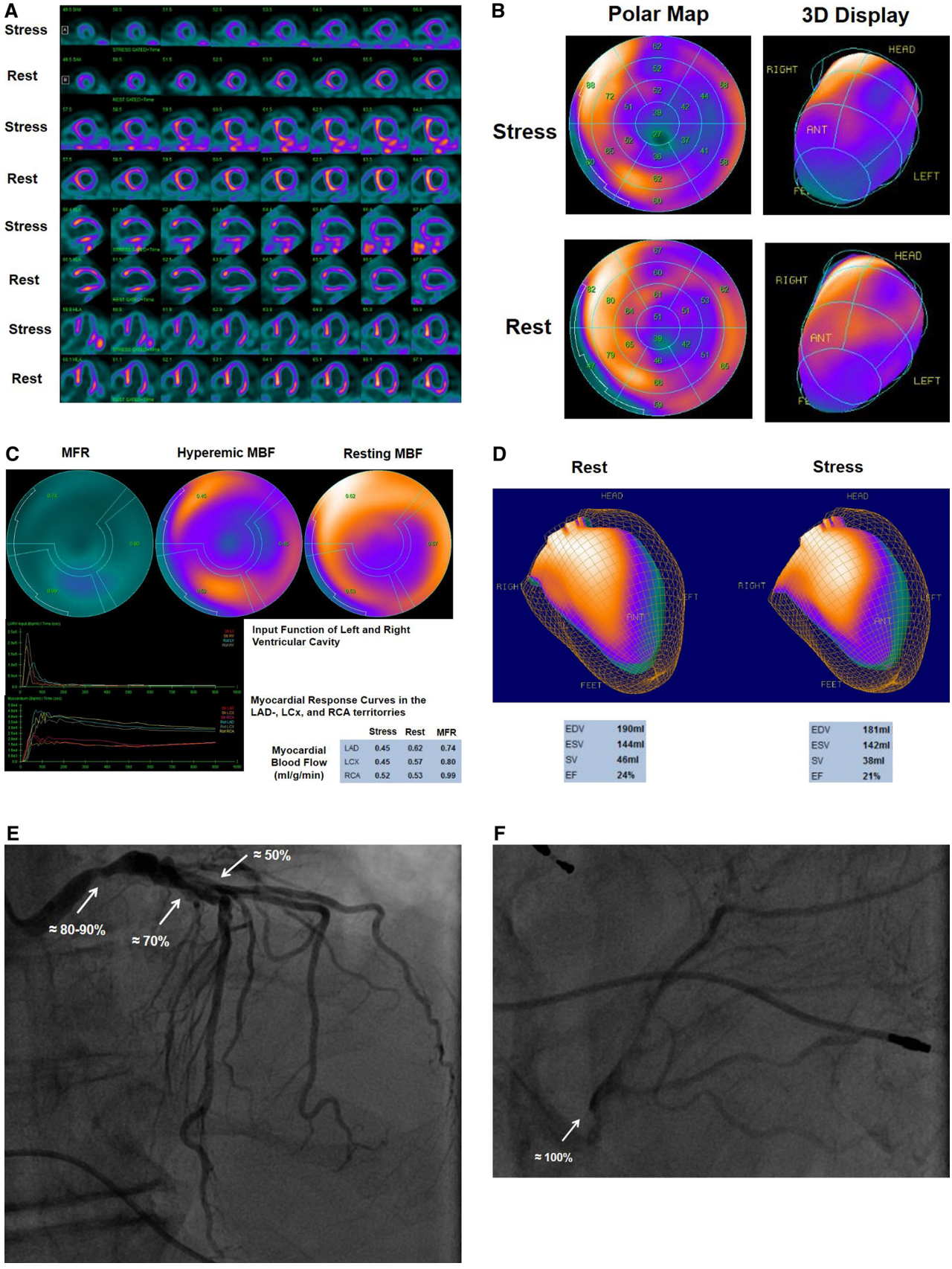
A
Stress
Rest
Stress
Rest
Stress
Rest
Stress
Rest
B
Polar Map
3D Display
Stress
Rest
HEAD
RIGHT
ANT
LEFT
C
MFR
Hyperemic MBF
Resting MBF
Input Function of Left and Right Ventricular Cavity
Myocardial Response Curves in the LAD-, LCx, and RCA territorries
Stress Rest MFR
Myocardial Blood Flow (ml/g/min)
LAD 0.45 0.62 0.74
LCX 0.45 0.57 0.80
RCA 0.52 0.53 0.99
D
Rest
Stress
HEAD
RIGHT
ANT
FEET
EDV 190ml
ESV 144ml
SV 46ml
EF 24%
EDV 181ml
ESV 142ml
SV 38ml
EF 21%
E
≈ 50%
≈ 80-90%
≈ 70%
F
≈ 100%

◀ **Figure 6.** ^{13}N-ammonia PET/CT-determined Perfusion, MBF, and wall motion with left main stem and multivessel disease. A 84-year-old man with known ischemic cardiomyopathy and known previous infarction presented with effort-induced chest tightness at minor exercise. (**A**) Rest ^{13}N-ammonia PET/CT images in corresponding short-axis (*top*), vertical long-axis (*middle*), and horizontal long-axis (*bottom*) slices display a heterogeneously reduced radiotracer uptake not only in the anterior, apical, and anterolateral but also in the infero-lateral wall with extension inferior indicative of previous myocardial infarction, which during vasomotor stress severely worsens and also extends to the inferoseptal and anteroseptal wall to signify diffuse ischemia of the left ventricle. (**B**) Corresponding display of myocardial perfusion on polar map and in 3D. (**C**) Regional myocardial blood flow quantification (MBF) and myocardial flow reserve (MFR) calculation with 13N-ammonia PET/CT and tracer kinetic modeling. The summarized quantitative data denote even a decrease of MBFs from rest to vasomotor stress and a MFR <1.0 in the LAD, LCx, and RCA distribution, respectively, which is widely specific for diffuse ischemia. (**D**) Global left ventricular ejection fraction (LVEF) on gated PET is severely reduced with 24% that slightly drops to 21% during peak stress signifying mild global myocardial stunning due to diffuse ischemia. (**E**) Invasive coronary angiography demonstrates a high grade lesion of the left main stem (≈80% to 90%) and intermediate lesions of the proximal LAD and LCx (≈70% to 80%). (**F**) The right coronary artery (RCA) is occluded in the periphery.

multicenter trial assessing the relationship between invasively measured coronary flow reserve and exercise-related ^{201}Thallium SPECT perfusion imaging in 55 patients with stenosis of intermediate severity (40% to 70%; mean value: 59% ± 12%).[72] A coronary flow reserve <1.7 predicted the presence of exercise-induced myocardial perfusion defect in 56 of 67 stenoses (agreement = 84%; kappa = 0.67; 95% CI = 0.48 to 0.86). The agreement further increased to 88% (46 of 52 stenoses) in patients who achieved 75% of their predicted maximum heart rate. Thus, several single-center studies[69-71] and on multicenter trial[72] have outlined a strong correlation between post-stenotic coronary flow velocity reserve and scintigraphic myocardial stress perfusion imaging, outlining that invasively or Doppler-derived coronary flow reserve accurately predicts the presence of exercise-induced ischemia on stress ^{201}Thallium perfusion imaging in CAD patients with epicardial narrowing of intermediate severity. Overall, these studies had high sensitivity (82% to 94%), specificity (92% to 100%), predictive accuracy (89% to 96%), and positive and negative predictive values (94% to 100% and 77% to 95%, respectively) (Table 3).

MFR VS HYPEREMIC MBF

Resting MBF in healthy volunteers may vary between 0.4 and 1.2 $mL \cdot g^{-1} \cdot min^{-1}$.[73-77] Apart from some variability related to methodological differences (different radiotracers, tracer kinetic models, and flow quantification), the variability of resting MBF in the individual person can be related to differences in left ventricular myocardial work load.[63,74,75] A close linear relationship between resting MBF and the rate pressure product (RPP = heart rate × systolic blood pressure), as an index for cardiac work and thus stringent on metabolic oxygen demand, has been described (Figure 2).[74,75,78] Such observations outline that increases in myocardial work load are paralleled by a corresponding flow increase to appropriately meet elevations in myocardial oxygen demand not only at rest but also during ''physical'' stress (e.g., bicycle or treadmill exercise, or dobutamine stimulation).[33,78] Resting MBF is commonly higher in patients with increases in heart rate or arterial hypertension since these conditions lead to an increase myocardial workload.[1,79-81] Similarly, resting MBF may also be elevated in advanced obesity due to more enhanced activation of the sympathetic nervous and renin-angiotensin-aldosterone system that again leads to higher resting heart rates and arterial blood pressures.[80-82] As regards age and gender, they may also impact resting flow as reported in several investigations.[74,75,83] The well-described age-related increase in resting MBF has been described to be paralleled by relative increases in systolic blood pressure, resulting in higher myocardial workload.[75,84] As regards gender, most PET flow studies report of higher resting flows in female than in male.[74,83,85,86] The exact causes of these differences remain uncertain but may be related, at least in part, to effects of estrogen on coronary vasomotor reactivity in women with CAD and/or gender-dependent lipid profile alterations.[21,87]

It is important to bear in mind that increases in resting MBF due to pronounced arterial hypertension, for example, however, can lead to reduced MFR (<2.0) although hyperemic MBFs during pharmacologic vasodilation, as determined with ^{13}N-ammonia PET/CT, may still be maintained (≥1.8 $mL \cdot g^{-1} \cdot min^{-1}$).[47] Under such condition, the decision to identify flow-limiting effects for a given epicardial stenosis ≥70% should be based on hyperemic MBF values and not on the MFR.[26] Conversely, patients presenting with bradycardia or previous subendocardial myocardial infarction may have low resting MBFs that again may lead to a ''pseudo''-normalization of the MFR, even if hyperemic MBFs are abnormally reduced (<1.8 $mL \cdot g^{-1} \cdot min^{-1}$). When interpreting the MFR, therefore, pronounced changes in resting flow due to alterations in metabolic demand need to be taken into account, and, if so, the clinical decision should be based on hyperemic MBFs that are not influenced by resting flow values.[6,61] Calculating the MFR (ratio of hyperemic to resting MBF), however, affords the advantage that any

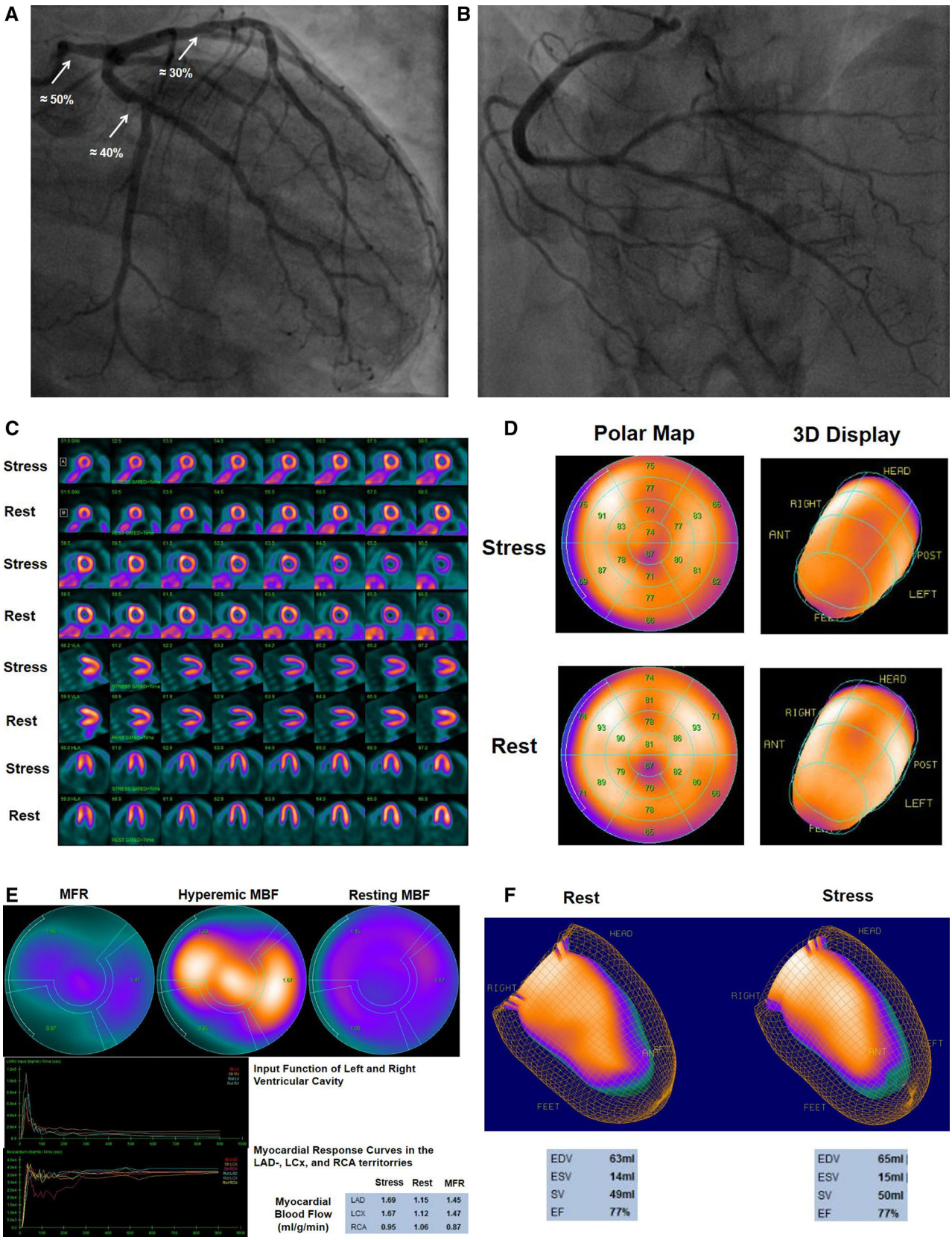
A
≈ 50%
≈ 30%
≈ 40%
B
C
Stress
Rest
Stress
Rest
Stress
Rest
Stress
Rest
D
Polar Map
3D Display
Stress
Rest
HEAD
RIGHT
ANT
POST
LEFT
E
MFR
Hyperemic MBF
Resting MBF
Input Function of Left and Right Ventricular Cavity
Myocardial Response Curves in the LAD-, LCx, and RCA territorries
Stress Rest MFR
Myocardial Blood Flow (ml/g/min)
LAD 1.69 1.15 1.45
LCX 1.67 1.12 1.47
RCA 0.95 1.06 0.87
F
Rest
Stress
HEAD
RIGHT
ANT
FEET
EDV 63ml
ESV 14ml
SV 49ml
EF 77%
EDV 65ml
ESV 15ml
SV 50ml
EF 77%

◀**Figure 7.** ^{13}N-ammonia PET/CT-determined perfusion, MBF, and wall motion with left main stem disease. A 38-year-old woman with arterial hypertension and dyslipidemia presented with exercise-related chest pain. (**A**) Invasive coronary angiography displays a proximal narrowing of ≈50% of the left main (LM) vessel. Furthermore, a 30% stenosis in the mid left anterior descending artery (LAD) after the first diagonal branch is noted, whereas a ≈40% narrowing is noted in the left circumflex artery (LCx) proximal to the second marginal branch. (**B**) The right coronary artery (RCA) system is free of CAD. (**C**) The patient was referred for ^{13}N-ammonia myocardial perfusion and flow PET/CT to evaluate the hemodynamic significance of the LM lesion. Regadenoson stress and rest ^{13}N-ammonia PET/CT images in corresponding short-axis (*top*), vertical long-axis (*middle*), and horizontal long-axis (*bottom*) slices demonstrate a widely homogenous and, thus, normal radiotracer uptake of the left ventricle. (**D**) Corresponding display of myocardial perfusion on polar map and in 3D. (**E**) Regional myocardial blood flow quantification (MBF) and myocardial flow reserve (MFR) calculation with 13N-ammonia PET/CT and tracer kinetic modeling. The summarized quantitative data denote reduced hyperemic MBFs (<1.85 mL·g^{-1}·min^{-1}) and myocardial flow reserve (MFR <2.0) in the LAD, LCx, and RCA distribution, respectively. (*Str*, stress; *Rst* rest; *LV*, left ventricle; *RV* right ventricle). (**F**) Since on gated PET left ventricular wall motion is normal associated with a left ventricular ejection fraction (LVEF) of 77% at rest and also at peak stress, respectively, diffuse myocardial ischemia potentially related to the left main lesion can be excluded. In the absence of a global hypokinesis during ''peak'' stress without a drop in LVEF during stress from rest, the marked reductions in hyperemic MBFs and MFR in all three major coronary territories do not reflect diffuse myocardial ischemia but rather represents cardiovascular risk factor-induced microvascular dysfunction (reproduced with permission from reference[26]).

methodological error that leads to under- or overestimation of MBFs will cancel out.[88-90] Thus, any systemic error in flow calculation may not count as long as the same percentage error is made both during hyperemic flow stimulation and at rest.[90] Nevertheless, applying the flow radiotracer ^{15}O-water and PET, recent clinical investigation by Danad et al[6] signifies hyperemic MBFs as determined to be more accurate in detecting flow-limiting stenoses on both per-patient and per-vessel analyses. Similar observations were reported by Hajjiri et al[47] with ^{13}N-ammonia and PET myocardial flow quantification. Hyperemic MBFs in response to adenosine stimulation had a higher sensitivity and comparable specificity in the detection of significant CAD as defined by ≥70% diameter stenosis (0.81 vs 0.62 and 0.82 vs 0.85, respectively), while the higher predictive accuracy did reach borderline significance (0.84 vs 0.79, $P = .06$). Given that hyperemic MBFs appear more accurate than MFR for the identification and characterization of flow-limiting CAD and, at the same time, independent of the resting MBF and its variation stringent to the myocardial workload condition, stress only PET assessment of hyperemic MBFs may be an alternative to stress-rest PET for perfusion and MFR calculation in describing the functional severity of epicardial lesions that warrants further investigations.[6,26,61]

IDENTIFICATION OF DIFFUSE ISCHEMIA

The conventional approach of myocardial scintigraphic perfusion imaging to evaluate the ''relative'' radiotracer uptake in the left ventricular myocardium may miss to detect ''balanced'' reductions of hyperemic MBF in the presence of significant left main lesion and/or three-vessel disease. The problem lies in the ''relative'' distribution of the radiotracer uptake since hyperemic MBF may be widely homogeneously decreased in the entire left ventricle without any detectable regional difference in radiotracer uptake.[91] For example, Lima et al[92] studied stress gated ^{99m}Technetium sestamibi SPECT to detect regional myocardial perfusion defects in 143 patients with angiographic three-vessel disease. The angiographic criteria for coronary three-vessel disease group were the presence of ≥50% narrowing of the internal diameter of left main coronary artery plus ≥70% narrowing of the right coronary artery or ≥70% narrowing of the left anterior descending artery, right coronary artery, and left circumflex artery, or their major branches. As it was observed, only in 10% (14/143) of patients with demonstrated three-vessel CAD stress-induced regional perfusion defects were indeed detected.[92] When regional wall motion abnormalities on post-stress gated SPECT were added to myocardial perfusion imaging, the identification of three-vessel CAD increased but only to 25%. Another study investigated 101 patients with significant left main CAD (≥50% stenosis) but without prior myocardial infarction or coronary revascularization, who underwent gated exercise or adenosine stress ^{99m}Technetium-sestamibi SPECT myocardial perfusion imaging.[93] Evaluating myocardial perfusion images, high-risk feature with moderate to severe perfusion defects (>10% myocardium at stress) was observed in up to 59%. On the other hand, no significant stress-related perfusion defect (≥5% myocardium) was noted in 13% to 15% of patients. When combining abnormal perfusion and wall motion on post-stress gated SPECT, however, the detection of high-risk individuals increased to 83%. To further optimize the detection of diffuse ischemia, the concurrent assessment of hyperemic MBF and MFR to perfusion with PET may be of help. Given the presence of significant left main lesion and/or three-vessel disease, reductions in hyperemic MBFs and MFR in all three major coronary

artery vascular territories of the LAD, LCx, and RCA are to be expected (Figures 3, 6). Someone could argue, however, that diffuse decreases of hyperemic MBFs and/or MFR are rather related to pronounced microvascular dysfunction than to significant left main lesion and/or three-vessel disease. For this reason, it is advisable to confirm stress-induced diffuse ischemia by a ''peak'' stress transient ischemic cavity dilation (TID) and associated global hypokinesis on gated PET images (Figure 3).[51,94]

Conversely, Naya et al[51] demonstrated that PET-determined normal hyperemic MBFs carry a high negative predictive value of 97% in excluding high-risk CAD on coronary angiography. Such information can also be reinforced by the evaluation of the left ventricular (LV) ejection reserve (ΔLVEF = stress LVEF − rest LVEF).[51] For the exclusion of significant left main and/or three-vessel CAD, a LVEF reserve of more than +5% had a positive predictive value of only 41% but a negative predictive value of 97%. Combining the information of normal hyperemic coronary flows and a normal to high LVEF reserve can widely rule out the presence of significant left main and/or three-vessel disease (Figure 7).[25,51] Overall, the combined evaluation of hyperemic MBFs, MFR, LVEF at ''peak'' stress as well as adding the LVEF reserve may indeed afford an accurate differentiation between significant left main and/or three-vessel CAD induced diffuse ischemia, its exclusion, and the presence of predominantly microvascular dysfunction (Figure 3).

In cardiomyopathy patients with low left ventricular function, however, the latter described scenario may not entirely hold true anymore. This is as ischemic preconditioning of the heart confers a certain cardioprotection that may prevent or delay a further worsening of left ventricular function despite repetitive episodes of myocardial ischemia.[95,96] Thus, despite stress-induced diffuse ischemia, only a minor or no further drop of LVEF is likely to ensue. In this setting, diffuse reductions in hyperemic MBFs in patients can reflect diffuse ischemia or just microvascular dysfunction. As a gated PET-determined drop in LVEF from stress to rest is unlikely to occur in these systolic heart failure patients, a definite differentiation between diffuse ischemia and microvascular dysfunction may not be possible (Figure 8). In such cases, non-invasive or invasive coronary angiography may be considered as subsequent step avoiding to miss high-risk CAD as underlying cause for ischemic cardiomyopathy. Conversely, as normal hyperemic MBFs also widely exclude high-risk CAD in heart failure patients,[25] further diagnostic evaluation with coronary angiography may not be needed any more.

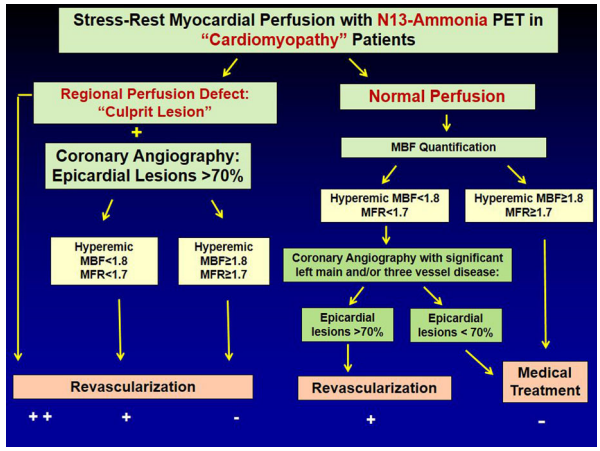

Figure 8. Algorithm for the integration of ^{13}N-ammonia PET/CT perfusion images, hyperemic MBFs and MFR in individuals with cardiomyopathy. Since in patients without cardiomyopathy or normal left ventricular function, a stress-induced regional perfusion defect signifies the ''culprit'' or most advanced CAD lesion, while hyperemic MBF and MFR may signify flow-limiting effects of lesions >70% diameter stenosis in patients with ischemic cardiomyopathy. Normal perfusion imaging, however, may not exclude diffuse ischemia due to significant left main and/or three-vessel disease. While normal hyperemic MBFs and MFRs may widely exclude high-risk CAD, this is not the case for abnormal hyperemic flows. Abnormal hyperemic MBFs may reflect diffuse microvascular function or diffuse ischemia in cardiomyopathy patients. In this setting, the additional wall motion analysis of the left ventricle at peak stress is not likely to be of much help as left ventricular function is severely reduced in most patients, and a further significant drop in left ventricular ejection fraction is not to be expected due to ischemic conditioning or cardioprotective effects. Thus, given normal perfusion but abnormal hyperemic MBFs in cardiomyopathy patients, invasive or non-invasive coronary angiography may be considered to triage these high-risk patients to coronary revascularization procedures or medical treatment alone.

SUMMARY

In the clinical setting, the concurrent ability of PET to non-invasively quantify MBF and LVEF at ''peak'' stress extends the scope of conventional myocardial perfusion imaging from the classical CAD detection to an optimized characterization of the extent and severity of ischemia in multivessel disease. In addition, combining myocardial perfusion, hyperemic MBF, and LVEF at ''peak'' stress affords the differentiation between diffuse ischemia owing to significant left main lesion and/or three-vessel disease, its exclusion, and the presence of predominantly microvascular dysfunction in cardiovascular risk individuals with normal left ventricular function. While the assessment of normal hyperemic MBFs widely rules out high-risk CAD in heart failure patients, reduced hyperemic MBFs may not differentiate

between diffuse ischemia and microvascular dysfunction as myocardial stunning may not necessarily result in a further drop in left ventricular function due to pre-ischemic conditioning. In the latter setting, non-invasive or invasive coronary angiography is recommended in order not to miss high-risk CAD. While the herein described different diagnostic scenarios interrelating CAD, perfusion, and MBF may be seen as intuitively correct, further evaluation in large scale clinical trials is certainly needed. PET/CT with the concurrent evaluation of myocardial perfusion, flow, and left ventricular function at peak stress, however, may emerge as pivotal tool to individualize and guide the decision-making process for coronary revascularization procedures in CAD patients in the near future.

Acknowledgment

This article was supported by a departmental fund from Johns Hopkins University, Baltimore, Maryland (No. 175470), and a research grant from the Swiss National Science Foundation (No. 3200N0-122237).

Disclosure

There is no relationship between industry and financial associations from within the past 2 years that might pose a conflict of interest in connection with the submitted article.

References

1. Schindler TH, Schelbert HR, Quercioli A, Dilsizian V. Cardiac pet imaging for the detection and monitoring of coronary artery disease and microvascular health. JACC Cardiovasc Imaging 2010;3:623-40.
2. Bengel FM. Leaving relativity behind: Quantitative clinical perfusion imaging. J Am Coll Cardiol 2011;58:749-51.
3. Schindler TH, Quercioli A, Valenta I, Ambrosio G, Wahl RL, Dilsizian V. Quantitative assessment of myocardial blood flow-clinical and research applications. Semin Nucl Med 2014;44:274-93.
4. Gould KL, Johnson NP, Bateman TM, Beanlands RS, Bengel FM, Bober R, et al. Anatomic versus physiologic assessment of coronary artery disease. Role of coronary flow reserve, fractional flow reserve, and positron emission tomography imaging in revascularization decision-making. J Am Coll Cardiol 2013;62:1639-53.
5. Danad I, Raijmakers PG, Harms HJ, Heymans MW, van Royen N, Lubberink M, et al. Impact of anatomical and functional severity of coronary atherosclerotic plaques on the transmural perfusion gradient: A [15O]H2O pet study. Eur Heart J 2014;35:2094-105.
6. Danad I, Uusitalo V, Kero T, Saraste A, Raijmakers MD, Lammertsma AA, et al. Quantitative assessment of myocardial perfusion in the detection of significant coronary artery disease. J Am Coll Cardiol 2014;64:1464-75.
7. Schindler TH, Nitzsche EU, Schelbert HR, Olschewski M, Sayre J, Mix M, et al. Positron emission tomography-measured abnormal responses of myocardial blood flow to sympathetic stimulation are associated with the risk of developing cardiovascular events. J Am Coll Cardiol 2005;45:1505-12.
8. Herzog BA, Husmann L, Valenta I, Gaemperli O, Siegrist PT, Tay FM, et al. Long-term prognostic value of 13N-ammonia myocardial perfusion positron emission tomography added value of coronary flow reserve. J Am Coll Cardiol 2009;54:150-6.
9. Ziadi MC, Dekemp RA, Williams KA, Guo A, Chow BJ, Renaud JM, et al. Impaired myocardial flow reserve on rubidium-82 positron emission tomography imaging predicts adverse outcomes in patients assessed for myocardial ischemia. J Am Coll Cardiol 2011;58:740-8.
10. Murthy VL, Naya M, Foster CR, Gaber M, Hainer J, Klein J, et al. Association between coronary vascular dysfunction and cardiac mortality in patients with and without diabetes mellitus. Circulation 2012;126:1858-68.
11. Murthy VL, Naya M, Foster CR, Hainer J, Gaber M, Di Carli G, et al. Improved cardiac risk assessment with noninvasive measures of coronary flow reserve. Circulation 2011;124:2215-24.
12. Murthy VL, Naya M, Foster CR, Hainer J, Gaber M, Dorbala S, et al. Coronary vascular dysfunction and prognosis in patients with chronic kidney disease. JACC Cardiovasc Imaging 2012;5:1025-34.
13. Marinescu MA, Loffler AI, Ouellette M, Smith L, Kramer CM, Bourque JM. Coronary microvascular dysfunction, microvascular angina, and treatment strategies. JACC Cardiovasc Imaging 2015;8:210-20.
14. Recio-Mayoral A, Rimoldi OE, Camici PG, Kaski JC. Inflammation and microvascular dysfunction in cardiac syndrome x patients without conventional risk factors for coronary artery disease. JACC Cardiovasc Imaging 2013;6:660-7.
15. Pries AR, Badimon L, Bugiardini R, Camici PG, Dorobantu M, Duncker DJ, et al. Coronary vascular regulation, remodelling, and collateralization: Mechanisms and clinical implications on behalf of the working group on coronary pathophysiology and microcirculation. Eur Heart J 2015;45:3134-46.
16. Crea F, Camici PG, Bairey Merz CN. Coronary microvascular dysfunction: An update. Eur Heart J 2014;35:1101-11.
17. Schindler TH, Cadenas J, Facta AD, Li Y, Olschewski M, Sayre J, et al. Improvement in coronary endothelial function is independently associated with a slowed progression of coronary artery calcification in type 2 diabetes mellitus. Eur Heart J 2009;30:3064-73.
18. Bravo PE, Tahari A, Pozios I, Luo HC, Bengel FM, Wahl RL, et al. Apparent left ventricular cavity dilatation during PET/CT in hypertrophic cardiomyopathy: Clinical predictors and potential mechanisms. J Nucl Cardiol 2015. doi:10.1007/s12350-015-0158-8.
19. Spoladore R, Maron MS, D'Amato R, Camici PG, Olivotto I. Pharmacological treatment options for hypertrophic cardiomyopathy: High time for evidence. Eur Heart J 2012;33:1724-33.
20. Quercioli A, Montecucco F, Pataky Z, Thomas A, Ambrosio G, Staub C, et al. Improvement in coronary circulatory function in morbidly obese individuals after gastric bypass-induced weight loss: Relation to alterations in endocannabinoids and adipocytokines. Eur Heart J 2013;34:2063-73.
21. Schindler TH, Campisi R, Dorsey D, Prior JO, Olschewski M, Sayre J, et al. Effect of hormone replacement therapy on vasomotor function of the coronary microcirculation in postmenopausal women with medically treated cardiovascular risk factors. Eur Heart J 2009;30:978-86.
22. Bravo PE, Di Carli MF. Does clopidogrel affect the efficacy of myocardial perfusion imaging? J Nucl Cardiol 2015. doi:10.1007/s12350-015-0280-7.
23. Valenta I, Dilsizian V, Quercioli A, Ruddy TD, Schindler TH. Quantitative PET/CT measures of myocardial flow reserve and atherosclerosis for cardiac risk assessment and predicting adverse patient outcomes. Curr Cardiol Rep 2013;15:344.

24. Valenta I, Quercioli A, Schindler TH. Diagnostic value of pet-measured longitudinal flow gradient for the identification of coronary artery disease. JACC Cardiovasc Imaging 2014;7:387-96.
25. Naya M, Murthy VL, Taqueti VR, Foster CR, Klein J, Garber M, et al. Preserved coronary flow reserve effectively excludes high-risk coronary artery disease on angiography. J Nucl Med 2014;55:248-55.
26. Schindler TH. Positron-emitting myocardial blood flow tracers and clinical potential. Prog Cardiovasc Dis 2015;57:588-606.
27. Gould KL, Kirkeeide RL, Buchi M. Coronary flow reserve as a physiologic measure of stenosis severity. J Am Coll Cardiol. 1990;15:459-74.
28. Gould KL, Lipscomb K. Effects of coronary stenoses on coronary flow reserve and resistance. Am J Cardiol. 1974;34:48-55.
29. Gould KL, Lipscomb K, Calvert C. Compensatory changes of the distal coronary vascular bed during progressive coronary constriction. Circulation. 1975;51:1085-94.
30. Gould KL, Lipscomb K, Hamilton GW. Physiologic basis for assessing critical coronary stenosis. Instantaneous flow response and regional distribution during coronary hyperemia as measures of coronary flow reserve. Am J Cardiol. 1974;33:87-94.
31. Uren NG, Melin JA, De Bruyne B, Wijns W, Baudhuin T, Camici PG. Relation between myocardial blood flow and the severity of coronary-artery stenosis. N Engl J Med. 1994;330:1782-8.
32. Di Carli M, Czernin J, Hoh CK, Gerbaudo VH, Brunken RC, Huang SC, et al. Relation among stenosis severity, myocardial blood flow, and flow reserve in patients with coronary artery disease. Circulation. 1995;91:1944-51.
33. Krivokapich J, Czernin J, Schelbert HR. Dobutamine positron emission tomography: Absolute quantitation of rest and dobutamine myocardial blood flow and correlation with cardiac work and percent diameter stenosis in patients with and without coronary artery disease. J Am Coll Cardiol. 1996;28:565-72.
34. Demer LL, Gould KL, Goldstein RA, Kirkeeide RL, Mullani NA, Smalling RW, et al. Assessment of coronary artery disease severity by positron emission tomography. Comparison with quantitative arteriography in 193 patients. Circulation. 1989;79:825-35.
35. Seiler C, Stoller M, Pitt B, Meier P. The human coronary collateral circulation: Development and clinical importance. Eur Heart J 2013;34:2674-82.
36. Meier P, Hemingway H, Lansky AJ, Knapp G, Pitt B, Seiler C. The impact of the coronary collateral circulation on mortality: A meta-analysis. Eur Heart J 2012;33:614-21.
37. Sato A, Hiroe M, Tamura M, Ohigashi H, Nozato T, Hikita H, et al. Quantitative measures of coronary stenosis severity by 64-slice ct angiography and relation to physiologic significance of perfusion in nonobese patients: Comparison with stress myocardial perfusion imaging. J Nucl Med 2008;49:564-72.
38. Beanlands RS, Muzik O, Melon P, Sutor R, Sawada S, Muller D, et al. Noninvasive quantification of regional myocardial flow reserve in patients with coronary atherosclerosis using nitrogen-13 ammonia positron emission tomography. Determination of extent of altered vascular reactivity. J Am Coll Cardiol. 1995;26:1465-75.
39. van de Hoef TP, Siebes M, Spaan JAE, Piek JJ. Fundamentals in clinical coronary physiology: Why coronary flow is more important than coronary pressure. Eur Heart J 2015. doi: 10.1093/eurheartj/ehv235.
40. Meier P, Gloekler S, Zbinden R, Beckh S, de Marchi SF, Zbinden S, et al. Beneficial effect of recruitable collaterals: A 10-year follow-up study in patients with stable coronary artery disease undergoing quantitative collateral measurements. Circulation 2007;116:975-83.
41. Seiler C, Engler R, Berner L, Stoller M, Meier P, Steck H, Traupe T. Prognostic relevance of coronary collateral function: Confounded or causal relationship? Heart 2013;99:1408-14.
42. Di Carli MF, Hachamovitch R. New technology for noninvasive evaluation of coronary artery disease. Circulation 2007;115:1464-80.
43. Schindler TH, Zhang XL, Vincenti G, Lerch R, Schelbert HR. Role of pet in the evaluation and understanding of coronary physiology. J Nucl Cardiol 2007;14:589-603.
44. Baller D, Notohamiprodjo G, Gleichmann U, Holzinger J, Weise R, Lehmann J. Improvement in coronary flow reserve determined by positron emission tomography after 6 months of cholesterol-lowering therapy in patients with early stages of coronary atherosclerosis. Circulation. 1999;99:2871-5.
45. Mancini GB, Henry GC, Macaya C, O'Neill BJ, Pucillo AL, Carere RG, et al. Angiotensin-converting enzyme inhibition with quinapril improves endothelial vasomotor dysfunction in patients with coronary artery disease. The trend (trial on reversing endothelial dysfunction) study. Circulation. 1996;94:258-65.
46. Shaw LJ, Berman DS, Maron DJ, Mancini GB, Hayes SW, Hartigan PM, et al. Optimal medical therapy with or without percutaneous coronary intervention to reduce ischemic burden: Results from the clinical outcomes utilizing revascularization and aggressive drug evaluation (COURAGE) trial nuclear substudy. Circulation 2008;117:1283-91.
47. Hajjiri MM, Leavitt MB, Zheng H, Spooner AE, Fischman AJ, Gewirtz H. Comparison of positron emission tomography measurement of adenosine-stimulated absolute myocardial blood flow versus relative myocardial tracer content for physiological assessment of coronary artery stenosis severity and location. JACC Cardiovasc Imaging 2009;2:751-8.
48. Cecchi F, Olivotto I, Gistri R, Lorenzoni R, Chiriatti G, Camici PG. Coronary microvascular dysfunction and prognosis in hypertrophic cardiomyopathy. N Engl J Med 2003;349:1027-35.
49. Kern MJ. Coronary physiology revisited: Practical insights from the cardiac catheterization laboratory. Circulation 2000;101:1344-51.
50. Lim MJ, Kern MJ. Coronary pathophysiology in the cardiac catheterization laboratory. Curr Probl Cardiol 2006;31:493-550.
51. Dorbala S, Vangala D, Sampson U, Limaye A, Kwong R, Di Carli MF. Value of vasodilator left ventricular ejection fraction reserve in evaluating the magnitude of myocardium at risk and the extent of angiographic coronary artery disease: A 82rb PET/CT study. J Nucl Med 2007;48:349-58.
52. De Bruyne B, Hersbach F, Pijls NH, Bartunek J, Bech JW, Heyndrickx GR, et al. Abnormal epicardial coronary resistance in patients with diffuse atherosclerosis but ''normal'' coronary angiography. Circulation 2001;104:2401-6.
53. Gould KL, Nakagawa Y, Nakagawa K, Sdringola S, Hess MJ, Haynie M, et al. Frequency and clinical implications of fluid dynamically significant diffuse coronary artery disease manifest as graded, longitudinal, base-to-apex myocardial perfusion abnormalities by noninvasive positron emission tomography. Circulation 2000;101:1931-9.
54. Sdringola S, Loghin C, Boccalandro F, Gould KL. Mechanisms of progression and regression of coronary artery disease by pet related to treatment intensity and clinical events at long-term follow-up. J Nucl Med 2006;47:59-67.
55. Schindler TH, Facta AD, Prior JO, Campisi R, Inubushi M, Kreissl MC, et al. PET-measured heterogeneity in longitudinal myocardial blood flow in response to sympathetic and pharmacologic stress as a non-invasive probe of epicardial vasomotor dysfunction. Eur J Nucl Med Mol Imaging 2006;33:1140-9.

56. Schindler TH, Zhang XL, Vincenti G, Nkoulou R, Just H, Dahlbom M, et al. Diagnostic value of pet-measured heterogeneity in myocardial blood flows during cold pressor testing for the identification of coronary vasomotor dysfunction. J Nucl Cardiol 2007;14:688-97.
57. Valenta I, Quercioli A, Vincenti G, Nkoulou R, Dewarrat S, Rager O, et al. Structural epicardial disease and microvascular function are determinants of an abnormal longitudinal myocardial blood flow difference in cardiovascular risk individuals as determined with PET/CT. J Nucl Cardiol 2010;17:1023-33.
58. Sdringola S, Patel D, Gould KL. High prevalence of myocardial perfusion abnormalities on positron emission tomography in asymptomatic persons with a parent or sibling with coronary artery disease. Circulation 2001;103:496-501.
59. Schindler TH, Facta AD, Prior JO, Cadenas J, Zhang XL, Li Y, et al. Structural alterations of the coronary arterial wall are associated with myocardial flow heterogeneity in type 2 diabetes mellitus. Eur J Nucl Med Mol Imaging 2009;36:219-29.
60. Chamuleau SA, Tio RA, de Cock CC, de Muinck ED, Pijls NH, van Eck-Smit BL, et al. Prognostic value of coronary blood flow velocity and myocardial perfusion in intermediate coronary narrowings and multivessel disease. J Am Coll Cardiol 2002;39:852-8.
61. Schindler TH, Dilsizian V. PET-determined hyperemic myocardial blood flow: Further progress to clinical application. J Am Coll Cardiol 2014;64:1476-8.
62. Schindler TH, Zhang XL, Prior JO, Cadenas J, Dahlbom M, Sayre J, et al. Assessment of intra- and interobserver reproducibility of rest and cold pressor test-stimulated myocardial blood flow with (13)n-ammonia and pet. Eur J Nucl Med Mol Imaging 2007;34:1178-88.
63. Sawada S, Muzik O, Beanlands RS, Wolfe E, Hutchins GD, Schwaiger M. Interobserver and interstudy variability of myocardial blood flow and flow-reserve measurements with nitrogen 13 ammonia-labeled positron emission tomography. J Nucl Cardiol. 1995;2:413-22.
64. Ferrari M, Schnell B, Werner GS, Figulla HR. Safety of deferring angioplasty in patients with normal coronary flow velocity reserve. J Am Coll Cardiol. 1999;33:82-7.
65. Kern MJ, Donohue TJ, Aguirre FV, Bach RG, Caracciolo EA, Wolford T, et al. Clinical outcome of deferring angioplasty in patients with normal translesional pressure-flow velocity measurements. J Am Coll Cardiol. 1995;25:178-87.
66. Fiechter M, Ghadri JR, Gebhard C, Fuchs TA, Pazhenkottil AP, Nkoulou RN, et al. Diagnostic value of 13N-ammonia myocardial perfusion pet: Added value of myocardial flow reserve. J Nucl Med 2012;53:1230-4.
67. Ziadi MC, Dekemp RA, Williams K, Guo A, Renaud JM, Chow BJ, et al. Does quantification of myocardial flow reserve using rubidium-82 positron emission tomography facilitate detection of multivessel coronary artery disease? J Nucl Cardiol 2012;19:670-80.
68. Kern MJ, Donohue TJ, Aguirre FV, Bach RG, Caracciolo EA, Ofili E, et al. Assessment of angiographically intermediate coronary artery stenosis using the doppler flowire. Am J Cardiol. 1993;71:26D-33D.
69. Miller DD, Donohue TJ, Younis LT, Bach RG, Aguirre FV, Wittry MD, et al. Correlation of pharmacological 99mtc-sestamibi myocardial perfusion imaging with poststenotic coronary flow reserve in patients with angiographically intermediate coronary artery stenoses. Circulation. 1994;89:2150-60.
70. Joye JD, Schulman DS, Lasorda D, Farah T, Donohue BC, Reichek N. Intracoronary doppler guide wire versus stress single-photon emission computed tomographic thallium-201 imaging in assessment of intermediate coronary stenoses. J Am Coll Cardiol. 1994;24:940-7.
71. Deychak YA, Segal J, Reiner JS, Rohrbeck SC, Thompson MA, Lundergan CF, et al. Doppler guide wire flow-velocity indexes measured distal to coronary stenoses associated with reversible thallium perfusion defects. Am Heart J. 1995;129:219-27.
72. Heller LI, Cates C, Popma J, Deckelbaum LI, Joye JD, Dahlberg ST, et al. Intracoronary doppler assessment of moderate coronary artery disease: Comparison with 201TL imaging and coronary angiography. Facts study group. Circulation. 1997;96:484-90.
73. Bergmann SR, Herrero P, Markham J, Weinheimer CJ, Walsh MN. Noninvasive quantitation of myocardial blood flow in human subjects with oxygen-15-labeled water and positron emission tomography. J Am Coll Cardiol. 1989;14:639-52.
74. Chareonthaitawee P, Kaufmann PA, Rimoldi O, Camici PG. Heterogeneity of resting and hyperemic myocardial blood flow in healthy humans. Cardiovasc Res 2001;50:151-61.
75. Czernin J, Muller P, Chan S, Brunken RC, Porenta G, Krivokapich J, et al. Influence of age and hemodynamics on myocardial blood flow and flow reserve. Circulation. 1993;88:62-9.
76. Tamaki N, Yonekura Y, Senda M, Kureshi SA, Saji H, Kodama S, et al. Myocardial positron computed tomography with 13n-ammonia at rest and during exercise. Eur J Nucl Med. 1985;11:246-51.
77. Senneff MJ, Geltman EM, Bergmann SR. Noninvasive delineation of the effects of moderate aging on myocardial perfusion. J Nucl Med. 1991;32:2037-42.
78. Krivokapich J, Smith GT, Huang SC, Hoffman EJ, Ratib O, Phelps ME, et al. 13N-ammonia myocardial imaging at rest and with exercise in normal volunteers. Quantification of absolute myocardial perfusion with dynamic positron emission tomography. Circulation. 1989;80:1328-37.
79. Schindler TH, Nitzsche EU, Munzel T, Olschewski M, Brink I, Jeserich M, et al. Coronary vasoregulation in patients with various risk factors in response to cold pressor testing: Contrasting myocardial blood flow responses to short- and long-term vitamin c administration. J Am Coll Cardiol 2003;42:814-22.
80. Quercioli A, Pataky Z, Montecucco F, Carballo S, Thomas A, Staub C, et al. Coronary vasomotor control in obesity and morbid obesity: Contrasting flow responses with endocannabinoids, leptin, and inflammation. JACC Cardiovasc Imaging 2012;5:805-15.
81. Quercioli A, Pataky Z, Vincenti G, Makoundou V, Di Marzo V, Montecucco F, et al. Elevated endocannabinoid plasma levels are associated with coronary circulatory dysfunction in obesity. Eur Heart J 2011;32:1369-78.
82. Motivala AA, Rose PA, Kim HM, Smith YR, Bartnik C, Brook RD, et al. Cardiovascular risk, obesity, and myocardial blood flow in postmenopausal women. J Nucl Cardiol 2008;15:510-7.
83. Duvernoy CS, Meyer C, Seifert-Klauss V, Dayanikli F, Matsunari I, Rattenhuber J, et al. Gender differences in myocardial blood flow dynamics: Lipid profile and hemodynamic effects. J Am Coll Cardiol. 1999;33:463-70.
84. Uren NG, Camici PG, Melin JA, Bol A, de Bruyne B, Radvan J, et al. Effect of aging on myocardial perfusion reserve. J Nucl Med. 1995;36:2032-6.
85. Duvernoy CS, Rattenhuber J, Seifert-Klauss V, Bengel F, Meyer C, Schwaiger M. Myocardial blood flow and flow reserve in response to short-term cyclical hormone replacement therapy in postmenopausal women. J Gend Specif Med 2001;4:21-7.
86. Prior JO, Schindler TH, Facta AD, Hernandez-Pampaloni M, Campisi R, Dahlbom M, et al. Determinants of myocardial blood flow response to cold pressor testing and pharmacologic vasodilation in healthy humans. Eur J Nucl Med Mol Imaging 2007;34:20-7.

87. Campisi R, Nathan L, Pampaloni MH, Schoder H, Sayre JW, Chaudhuri G, et al. Noninvasive assessment of coronary microcirculatory function in postmenopausal women and effects of short-term and long-term estrogen administration. Circulation 2002;105:425-30.
88. Bacharach SL, Cuocolo A, Bonow RO. Arterial blood concentration curves by cardiac PET without arterial sampling or image reconstruction. Computers in Cardiology 1988. Washington: IEEE Computer Society Press; 1989.
89. Knuuti J, Saraste A. Advances in clinical application of quantitative myocardial perfusion imaging. J Nucl Cardiol 2012;19:643-6.
90. Bettencourt N, Chiribiri A, Schuster A, Ferreira N, Sampaio F, Pires-Morais G, et al. Direct comparison of cardiac magnetic resonance and multidetector computed tomography stress-rest perfusion imaging for detection of coronary artery disease. J Am Coll Cardiol 2013;61:1099-107.
91. Beller GA. Underestimation of coronary artery disease with spect perfusion imaging. J Nucl Cardiol 2008;15:151-3.
92. Lima RS, Watson DD, Goode AR, Siadaty MS, Ragosta M, Beller GA, et al. Incremental value of combined perfusion and function over perfusion alone by gated spect myocardial perfusion imaging for detection of severe three-vessel coronary artery disease. J Am Coll Cardiol 2003;42:64-70.
93. Berman DS, Kang X, Slomka PJ, Gerlach J, de Yang L, Hayes SW, et al. Underestimation of extent of ischemia by gated spect myocardial perfusion imaging in patients with left main coronary artery disease. J Nucl Cardiol 2007;14:521-8.
94. Dorbala S, Hachamovitch R, Curillova Z, Thomas D, Vangala D, Kwong RY, et al. Incremental prognostic value of gated rb-82 positron emission tomography myocardial perfusion imaging over clinical variables and rest lvef. JACC Cardiovasc Imaging 2009;2:846-54.
95. Heusch G. Cardioprotection: Chances and challenges of its translation to the clinic. Lancet 2013;381:166-75.
96. Heusch G, Botker HE, Przyklenk K, Redington A, Yellon D. Remote ischemic conditioning. J Am Coll Cardiol 2015;65:177-95.